Structural phase transitions in $CaSi_2$ under high pressure

P. Bordet
Laboratoire de Cristallographie, CNRS, Boîte Postale 166 Cedex 09, 38042 Grenoble, France

M. Affronte
Istituto Nazionale per la Fisica della Materia and Dipartamento di Fisica, Università di Modena e Reggio Emilia, via G. Campi, 213/A, 41100 Modena, Italy

S. Sanfilippo, M. Núñez-Regueiro, and O. Laborde
Centre de Recherches sur les Très Basses Températures, CNRS, Boîte Postale 166 Cedex 09, 38042 Grenoble, France

G. L. Olcese and A. Palenzona
Istituto Nazionale per la Fisica della Materia and Dipartamento di Chimica e Chimica Industriale, Università di Genova, via Dodecaneso 31, 16146 Genova, Italy

S. LeFloch
Laboratoire de Cristallographie, CNRS, Boîte Postale 166 Cedex 09, 38042 Grenoble, France

D. Levy and M. Hanfland
European Synchrotron Radiation Facility, Boîte Postale 220, 38043 Grenoble, France
(Received 31 March 2000; revised manuscript received 23 May 2000)

In situ x-ray-diffraction measurements under high pressure (P up to 20 GPa) have been used to study structural changes in the rhombohedral and the tetragonal phases of $CaSi_2$ at room temperature. Lattice parameters of the tetragonal phase regularly change with increasing pressure while the rhombohedral phase undergoes two structural phase transitions: A trigonal structure is observed for $9<P<16$ GPa and a new AlB_2-like phase appears for $P>16$ GPa. These observations lead to ascribe the appearance of superconductivity to the trigonal phase while the highest T_c's can be related to the transition towards the AlB_2-like phase that differs from the low-pressure phases by the almost planar bonds of silicon.

INTRODUCTION

Silicides are widely used in microelectronic as materials for interconnects of silicon-based devices. Besides such applications, the intercalation of metals with silicon layers, typical of silicides, has attracted much interest due to the possibility of tuning the silicon bonds and the electronic doping. Quite often, silicides present different polymorphs of the same stoichiometric composition that differ in the silicon (and/or the metal) coordination. Most of the studies have been focused on the interfaces between the silicon surfaces and silicides, with much emphasis on the electronic properties as well as on the growth of different polymorphs under different thermodynamic conditions. In order to have some control on the electronic properties, it is, however, mandatory to study the structural arrangements in which silicon may assume different coordinations. For what concerns bulk materials, it has been shown that pressure can be a powerful tool in order to obtain different structural phases and elementary silicon can be taken as an example: It may assume at least ten different structures under pressure.[1] It turns out that pressure can be effectively used to tune both structural and physical properties of metal-silicon compounds.

When prepared at ambient pressure, $CaSi_2$ has a rhombohedral structure (space group $R\bar{3}m$, $a\approx3.85$ Å, $c\approx30.62$ Å, belonging to the trigonal system, that is why quite often it is also named the ''*trigonal* $CaSi_2$ phase'' in the literature) in which double layers of diamondlike silicon atoms alternate with simple Ca atom sheets [Fig. 1(a)]. Rhombohedral $CaSi_2$ is a semimetal[2] in which the Si atoms form sp^3 bonds and both the Ca d electronic levels as well as the hybridization of the Si and the Ca orbitals are present at the Fermi level. By submitting this rhombohedral compound to annealing under pressure, a tetragonal (α-$ThSi_2$-type) phase is obtained[3] [space group $I4_1/amd$, $a\approx4.3$ Å, $c\approx13.5$ Å, Fig. 1(b)] in which the Si atoms are connected by a three-dimensional network of sp^2 bonds. Tetragonal $CaSi_2$ is superconducting with $T_c=1.58$ K. However, other polymorphs of this compound have been predicted to exist due to the fact that the energy cost for passing from one atom packing to another was estimated to be of the order of the ambient thermal energy.[4] Interestingly another $CaSi_2$ rhombohedral phase with $c\sim15$ Å was reported[5] and an AlB_2-type structure, separated by small energy barriers from the most stable rhombohedral structure, has been also predicted.[6]

The phase diagram of $BaSi_2$ compound has been recently studied in detail[7,8] and a superconducting transition at 6.8 K (Ref. 9) was found in a trigonal and metallic phase synthesized at high pressure and temperature. In a recent work[10] we have shown that starting from the rhombohedral $CaSi_2$ and applying high pressure it is possible to observe superconducting transitions with T_c up to 14 K and the appearance of

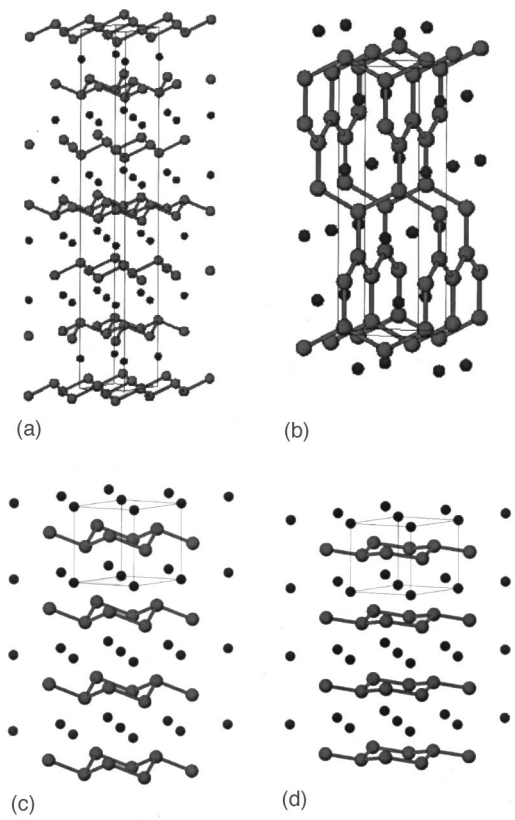

FIG. 1. Crystal structure of $CaSi_2$. (a) the rhombohedral phase, (b) the tetragonal phase, (c) the trigonal phase, and (d) the AlB_2-type phase.

superconductivity in this material is still a puzzling issue. The aim of the present work is twofold: to explore the phase diagram of $CaSi_2$ as a function of pressure and at room temperature, secondly to clarify which structure and which silicon arrangement gives rise to its enhanced superconductivity.

EXPERIMENTAL TECHNIQUES

The preparation of polycrystalline samples of rhombohedral $CaSi_2$ is described in Ref. 2. Briefly, high-purity Ca and Si in stoichiometric proportions were melted in a tantalum crucible closed by arc welding under inert gas atmosphere and, in order to obtain a homogeneous single phase intermetallic compound, samples were annealed for 7 days at 900 °C. X-ray diffraction and micrographic analysis confirmed that the samples were a single phase ($R\bar{3}m$ space group). Sample of the tetragonal $CaSi_2$ phase was prepared by using the heat treatment at high pressure described by Everts[3] in a belt-type apparatus, starting from the rhombohedral phase.

High-pressure diffraction experiments were performed at the ID09 beam line of the *European Synchrotron Radiation Facility* in Grenoble. The high-pressure conditions were obtained by using a diamond-anvil cell in combination with a ruby luminescence method[11] for pressure measurements. Nitrogen was used as pressure transmitting medium. X rays from an undulator source were focused vertically by a Pt coated Si mirror and horizontally by an asymmetrically cut

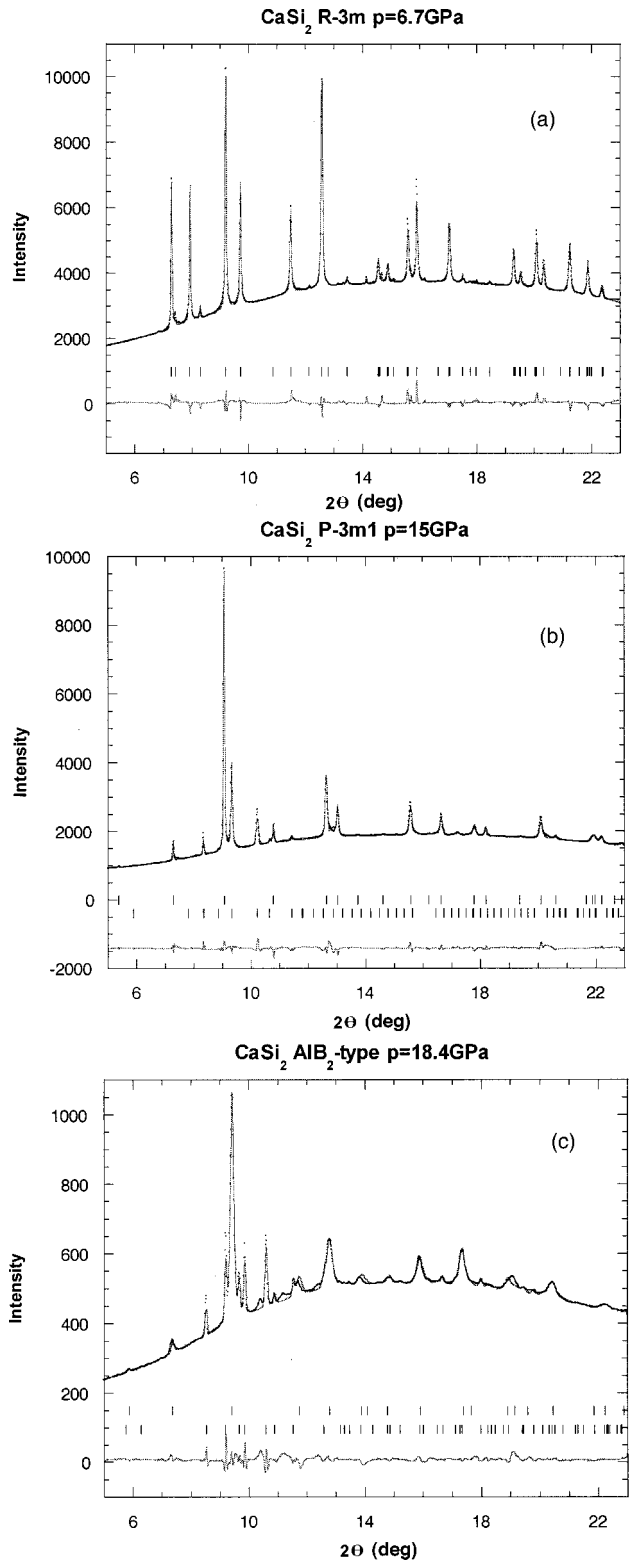

FIG. 2. Rietveld refinement plots of the diffraction patterns obtained at 6.7 GPa (a), 15 GPa (b), 18.4 GPa (c). The secondary phases indicated in (b) and (c) are solid molecular nitrogen. The upper ticks at the bottom of the figures mark the nitrogen phase while the lower ticks mark the $CaSi_2$ phases.

bent Si(111) Laue monochromator. Monochromatic radiation with wavelength of 0.413 18 Å was used and diffraction patterns were collected, after typical exposure time of 1–2 min, on an A3-size Fuji image plate located at ≈40 cm from the

TABLE I. Crystal structure parameters for the starting $CaSi_2$ rhombohedral phase as a function of the applied pressure. The normalized values correspond to a single formula unit, i.e., the *c* parameter and volume have been divided by 6 for the low-pressure phase.

Pressure (GPa)	*a* (Å)	*c* (Å)	Normalized *c* (Å)	Volume (Å^3)	Normalized volume (Å^3)	*z*(Ca) (Å)	*z*(Si1) (Å)	*z*(Si2) (Å)
0.6	3.8494(1)	30.544(19)	5.0906(2)	391.96	65.327	0.0827(3)	0.1832(3)	0.3447(3)
3.1	3.8149(1)	29.981(14)	4.9968(2)	377.87	62.978	0.0819(2)	0.1861(3)	0.3450(2)
5.0	3.7927(1)	29.632(15)	4.9387(2)	369.13	61.522	0.0812(3)	0.1862(3)	0.3458(3)
6.7	3.7730(1)	29.316(12)	4.8860(2)	361.41	60.235	0.0796(2)	0.1856(3)	0.3466(3)
9.8	3.7808(1)	4.5904(3)	4.5904(3)	56.827	56.827			0.3990(1)
10.6	3.7756(1)	4.5616(3)	4.5616(3)	56.315	56.315			0.3990(1)
11.7	3.7717(1)	4.5155(3)	4.5155(3)	55.629	55.629			0.402(1)
12.8	3.7668(2)	4.4752(3)	4.4752(3)	54.990	54.990			0.408(1)
13.9	3.7626(2)	4.4366(3)	4.4366(3)	54.396	54.396			0.408(1)
15.0	3.7554(1)	4.3951(3)	4.3951(3)	53.680	53.680			0.4124(9)
18.4	3.7112(3)	4.0391(7)	4.0391(7)	48.179	48.179			0.440(1)
19.3	3.7077(3)	4.0277(6)	4.0277(6)	47.951	47.951			0.448(1)

sample. The plates were scanned on a Molecular Dynamics image plate reader, and processed by using the FIT2D software.[12] The images were corrected for spatial distortion effects, and tilt corrections and wavelength/distance calibrations were obtained from standard silicon powder images. After removal of spurious peaks the corrected images were averaged over 360° about the direct beam position, yielding Intensity vs 2θ spectra. These data were then analyzed by the Rietveld technique, using the FULLPROF software. The background was modelled with a fifth-order polynomial, and the peak shape by a pseudo-Voigt function. Positional and isotropic thermal parameters were refined at each pressure point. On increasing pressure, several phases of solid molecular nitrogen also appeared: the cubic δ-N_2 phase between 5 and 11 GPa, the tetragonal δ^*-N_2 phase between 11 and 16 GPa, and the rhombohedral ε-N_2 phase above 16 GPa. These phases were taken into account by the cell constraint refinement technique, and only their cell and profile parameters and Bragg peak intensities were refined.

RESULTS

The evolutions of the diffraction pattern as a function of pressure were studied on two different samples of the rhombohedral $CaSi_2$ phase and one sample of the tetragonal phase at room temperature. Experiments were performed by taking diffraction spectra at regularly spaced values of increasing pressure. In the first set of experiments we used the rhombohedral $CaSi_2$ samples as starting material. Figure 2 shows three of the most representative x-ray-diffraction patterns obtained at different pressures (6.7, 15.0, and 18.4 GPa, respectively), together with the fits obtained by the refinement procedure. In the plots of Figs. 2(b) and (c), diffraction peaks (labeled by the upper ticks at the bottom of each figure) can be seen from the δ^*-N_2 and ε-N_2 phases, respectively. The refined structural parameters as well as selected interatomic distances and bond angles are reported in Tables I and II. The pressure dependence of the relative cell parameters are shown in Fig. 3, and the change of the bond distances and angles between silicon atoms are shown in Fig. 4.

In the 0–7-GPa pressure range, the structure undergoes a smooth volume contraction. However, a strong anisotropy of compressibility is observed along the *a* and *c* directions, the latter being about twice more compressible (3.25×10^{-3} and 6.58×10^{-3} GPa^{-1}, respectively). The distances and angles between silicon atoms remain almost constant, and most of the *c*-axis compression can be attributed to the reduction of

TABLE II. Principal interatomic distances and angles for the starting $CaSi_2$ rhombohedral phase as a function of the applied pressure.

Pressure (GPa)	*d*(Ca-Si1) (Å)	*d*(Ca-Si1) (Å)	*d*(Ca-Si2) (Å)	*d*(Si1-Si1) (Å)	*d*(Si2-Si2) (Å)	(Si1-Si1-Si1) angle (deg)	(Si2-Si2-Si2) angle (deg)
0.6	3.0681(138)	3.0291(94)	3.11(1)	2.441(6)	2.328(4)	104.1(2)	111.560(134)
3.1	3.1231(100)	2.9469(67)	3.048(6)	2.492(5)	2.311(3)	99.9(2)	111.230(99)
5.0	3.1116(118)	2.9328(79)	2.991(7)	2.478(6)	2.311(3)	99.8(2)	110.290(117)
6.7	3.1081(104)	2.9562(70)	2.920(6)	2.445(5)	2.312(4)	101.(2)	109.350(127)
9.8	2.8495(31)			2.372(3)		105.7(1)	
10.6	2.8397(30)			2.367(3)		105.8(1)	
11.7	2.8355(29)			2.350(2)		107.7(1)	
12.8	2.8396(31)			2.326(2)		108.2(1)	
13.9	2.8263(27)			2.322(2)		108.2(1)	
15.0	2.8260(25)			2.301(2)		109.4(1)	
18.4	2.7826(34)			2.198(2)		115.2(1)	
19.3	2.7990(39)			2.182(2)		116.3(1)	

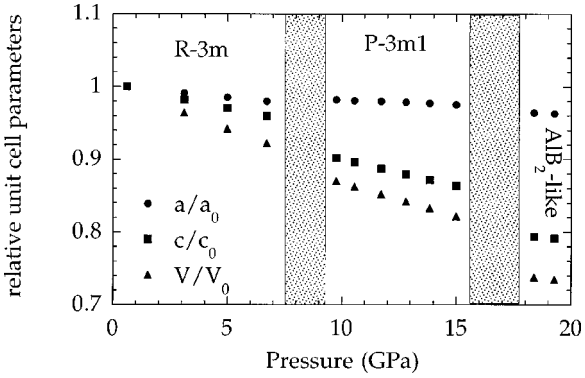

FIG. 3. Pressure dependence of the a and the normalized (i.e., for one formula unit) c axis and unit-cell volume measured at ambient temperature on the starting rhombohedral $CaSi_2$ phase. Two-phase regions have been hatched.

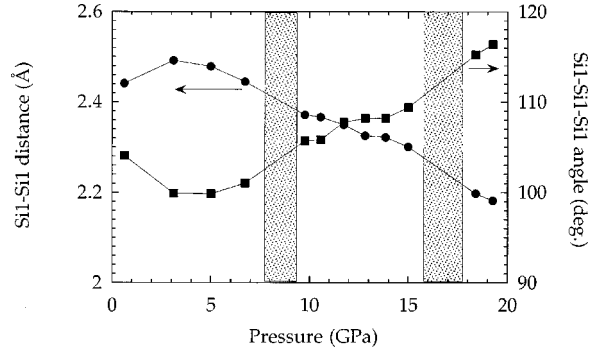

FIG. 4. Pressure dependence of the Si(1)-Si(1)-Si(1) angle and the Si(1)-Si(1) distance. Two-phase regions have been hatched.

the separation between the Ca and Si layers, leading to about 2.5% decrease of the average Ca-Si bond length.

The data can be refined with the rhombohedral $CaSi_2$ structure up to ≈7 GPa, above which a phase transition occurred, as can be clearly seen from a comparison of Figs. 2(a) and (b). Between ≈7 and 9.5 GPa, the two phases coexist in the sample, probably because of pressure inhomogeneity. This phase transition consists in a change from the rhombohedral structure ($R\bar{3}m$, $a_R \approx 3.77$ Å, $c_R \approx 29.32$ Å, $Z=6$) to a trigonal phase ($P\bar{3}m1$, $a_T \approx 3.78$ Å, $c_T \approx c_R/6 \approx 4.59$ Å, $Z=1$) with Ca at the $1a(0\,0\,0)$ position and Si at the $2d$ ($\frac{1}{3}\ \frac{2}{3}\ z \approx 0.4$) position [Fig. 1(c)]. This phase is very similar to the trigonal one of $BaSi_2$ synthesized at high-pressure and high-temperature conditions.[8] There are no major changes in the distances and angles between silicon atoms across the transition. On the other hand, the average Ca-Si distance strongly decreases from 2.99 Å at 6.7 GPa to 2.85 Å at 9.8 GPa. The driving force for this rhombohedral to trigonal phase transition can be interpreted as the need to adopt a more compact stacking as a response to the pressure-induced volume contraction, while the sp^3-like arrangement of the silicon sheets is conserved. Between 10 and 15 GPa, the a- and c-axis compressibility becomes highly anisotropic (1.28×10^{-3} and 8.13×10^{-3} GPa^{-1}, respectively). Contrary to what was observed in the low-pressure phase, the volume contraction is here mostly taken by a deformation of the silicon sheets. The main effect is the decrease by 0.15 Å of the distance between adjacent Si layers, while that between Ca and Si layers decreases only by 0.02 Å. As a consequence, the Si-Si distance decreases by 0.07 Å and the Si-Si-Si bond angle increases from 106° to 109°, still preserving a sp^3-like arrangement.

The trigonal symmetry is preserved on increasing pressure until a second phase transition occurs at ≈16 GPa. Here again, a region with the coexistence of two phase is observed between 16 and 18 GPa. The transition mainly consists in an abrupt decrease of c-lattice parameter (and unit-cell volume) by ≈10%. This is accompanied by a strong broadening of the diffraction peaks, which might be attributed to the concomitant phase transition from the δ^*-N_2 phase to the ε-N_2 phase, the latter being much harder, and consequently a far worse transmitting medium. Defects and stacking faults due to the phase transition in $CaSi_2$ can also contribute to the broadening of the diffraction peaks although we did not observe any marked anisotropy in the reflection broadening. The $CaSi_2$ high-pressure phase structure can still be refined in the $P\bar{3}m1$ symmetry, showing a marked increase of the Si z parameter from ≈0.4 to ≈0.44 [Fig. 1(d)]. The Si atom displacement leads to a strong decrease of the Si layer separation, from 0.7 to 0.4 Å which can account for the c-axis discontinuity. The Ca-Si distance slightly decreases by 0.04 Å across the transition. The major modification, however, is the increase of the Si-Si-Si bond angle from 109° to ~115°, accompanied by the Si-Si bond length decrease from 2.3 to 2.2 Å. These changes suggest that the bonding between the Si atoms may switch from sp^3- to sp^2-type as the Si sheets get flat. This phase may also be described as an AlB_2-type

TABLE III. Lattice parameters of the tetragonal $CaSi_2$ phase as a function of applied pressure.

P (GPa)	a (Å)	a/a_0	c (Å)	c/c_0	Volume (Å^3)	V/V_0
0.61200	4.2708±0.0001	1.0000	13.523±0.0001	1.0000	246.66±0.0003	1.00000
2.0000	4.2328±0.0001	0.99110	13.468±0.0005	0.99596	241.31±0.0008	0.97829
4.0300	4.1850±0.0001	0.97991	13.398±0.0005	0.99075	234.65±0.0008	0.95132
5.9700	4.1423±0.0001	0.96991	13.337±0.0005	0.98625	228.84±0.0007	0.92777
8.0600	4.1028±0.0001	0.96066	13.282±0.0007	0.98219	223.58±0.0009	0.90642
10.120	4.0632±0.0001	0.95139	13.231±0.0009	0.97842	218.44±0.0011	0.88560
12.010	4.0349±0.0001	0.94476	13.190±0.0009	0.97538	214.74±0.0011	0.87059
13.880	4.0053±0.0001	0.93783	13.157±0.0009	0.97294	211.07±0.0011	0.85572
15.960	3.9728±0.0002	0.93022	13.122±0.0011	0.97032	207.10±0.0015	0.83962
17.820	3.9442±0.0003	0.92353	13.099±0.0017	0.96863	203.77±0.0023	0.82613

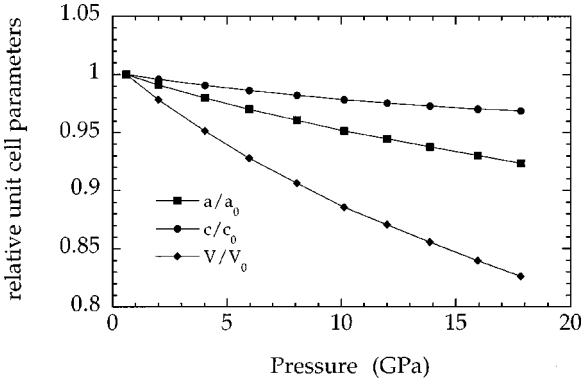

FIG. 5. Relative variations with pressure of the *a* and *c* parameters and unit-cell volume for the starting tetragonal $CaSi_2$ phase.

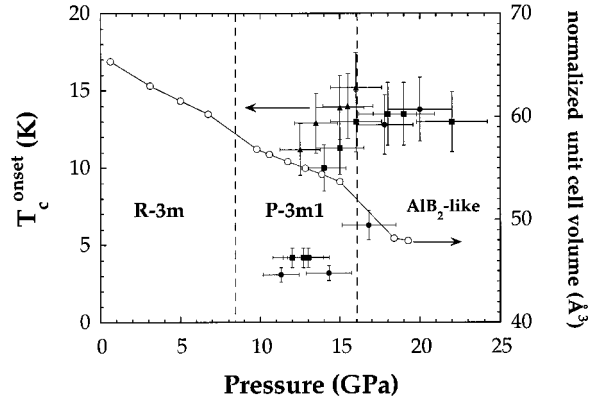

FIG. 6. Comparison of the pressure dependence of the superconducting transition temperature T_c^{onset} (from Ref. 10) with the structural phase diagram of $CaSi_2$ deduced by this work. Different symbols for the T_c's refer to distinct samples from the same batch.

structure, for which $z \approx \frac{1}{2}$. Note that for $z(\mathrm{Si}) = \frac{1}{2}$, the symmetry would become hexagonal, space group $P6/mmm$ with Ca at $1a$ (0 0 0) and Si at $2d$ ($\frac{1}{3}\ \frac{2}{3}\ \frac{1}{2}$). Refinements carried out with this hexagonal space group lead to slightly worse ($R_{\mathrm{Bragg}} = 8.7\%$, compared to 7.4%), but still satisfactory agreement factors. Taking into account the poor quality of data at the highest pressure, it would be reasonable to assume that this high-pressure phase has hexagonal symmetry. In the ideal case, i.e., the AlB_2-type structure, the Si layers would be flat by symmetry, with 120° bond angles and 2.14 Å bond lengths. Due to this similarity we name this high-pressure phase AlB_2-like, although, even at 20 GPa there is still a nonvanishing buckling of the Si planes.

The pressure dependence of the lattice parameter was also studied on the tetragonal $CaSi_2$ phase up to 18 GPa. This structure is built up by a Ca atom at ($0\ \frac{3}{4}\ \frac{1}{8}$), and a Si atom at ($0\ \frac{3}{4}\ z \approx 0.71$). The Rietveld refinements as function of pressure indicate a continuous decrease of the lattice parameters with increasing pressure, as reported in Table III and shown in Fig. 5. The *a*- and *c*-axis compressibilities are markedly anisotropic, with room-pressure values of 6.410^{-3} and $2.910^{-3}\,\mathrm{GPa}^{-1}$, respectively. No structural phase transition was observed up to 18 GPa, and the *z* parameter of the Si atom remains constant in the whole pressure range. This corresponds to a decrease of the average Si-Si bond length from 2.36 to 2.23 Å in the pressure range investigated. We remind that the tetragonal $CaSi_2$ phase is superconducting at ambient pressure and T_c^{onset} achieves a maximum ~6.5 K for 9 GPa.[10]

DISCUSSION

Two important structural transitions have been observed on the starting rhombohedral phase at $P \sim 9$ GPa and $P \sim 16$ GPa, respectively. The trigonal phase (space group D_{3d}^3 ($P\bar{3}m1$) observed between 9 and 16 GPa has been observed as a metastable phase grown in thin-film form.[13]

The trigonal $CaSi_2$ phase is the simplest structure presenting corrugated Si layers, which are essentially a section of the diamondlike structure of Si parallel to the (111) plane, alternated by Ca layers in the simple *AA* staking sequence [Fig. 1(c)]. In the rhombohedral room-pressure structure the Si planes are both shifted and rotated with respect to each other and the staking sequence is *AABBCC* in this case [Fig. 1(a)]. The structural phase transition from the rhombohedral to the trigonal structure can be simply regarded as a shift of the Si planes which ends up with an increase of the symmetry of the Ca-Si stacking sequence. Fahy and Hamann[4] have estimated that the energy barrier between the rhombohedral (named TR6 in Ref. 4) and the trigonal phase is of the order of 10 meV. They actually noticed that it matters little, for what concerns the energy of the system, whether the Ca ions are in a tetrahedral site (as in the rhombohedral phase) or in a hexagonal site (as in the trigonal phase) with respect to the Si layers. Therefore the fact that a phase transition takes place at room temperature under pressure should not be surprising. Kusakabe and co-workers[6] have discussed in detail the relative stability of the polymorphs by varying the external pressure. They show how the structure with sp^2 bonds of Si can actually be more stable at high pressure and predict that the AlB_2-type can be observed at high pressure, consistently to what we report in this work.

From an electronic point of view, Fahy and Hamann[4] showed that the Fermi surface of $CaSi_2$ consists of a hole pocket due to the (Ca)d-(Si)p hybridization and of smaller pockets of heavier electrons, primarily (Ca)d in character. The Si-Ca bond has a dominant covalent character[14] and this favors the shearing shift of the Si layers with respect to the Ca one. The shape of the electron part slightly depends on the stacking sequence of the Ca and Si layers while the hole part does not change much passing from the rhombohedral to the trigonal phase. On the other hand, preliminary results of band structure calculations[15] indicate that the density of electronic states at the Fermi level significantly increases by reducing the buckling of the Si planes, i.e., passing from the trigonal to the AlB_2-type structure. We may also expect at this transition a softening of phonon modes associated to the collapse of the corrugated Si planes. Both these facts can be relevant for the enhancement of the superconducting transition temperature T_c.

In a previous work we have shown that starting from the semimetallic rhombohedral $CaSi_2$, superconductivity occurs at high pressure.[10] Onset of the superconducting transition temperature T_c^{onset} of the order of 3–4 K were observed for pressure ranging between 11 and 14 GPa while for higher pressure (14 GPa up to 20 GPa) T_c^{onset} increases up to 14 K. In Fig. 6 we report the different T_c's measured as a function

of the applied pressure on three samples of the starting rhombohedral $CaSi_2$. The dependence of T_c vs P can be compared with the structural phase diagram deduced by this work. It turns out that at low pressure the rhombohedral phase is not superconducting. Superconductivity is observed for $P > 11$ GPa and it should be ascribed to the structural phase transition from the rhombohedral to the trigonal phase. The highest T_c's are however observed for $P > 14$ GPa. Taking into account that the transmitting medium was different in the two experiments (it is likely that the conditions were more hydrostatic in the diffraction than in the resistive experiments) and also the uncertainties in pressure determination, we are led to conclude that the T_c enhancement is related to the incipient structural transition. It is worth noticing that quite often superconductivity seems to be enhanced on silicon based materials when the Si bonding changes from sp^3 to sp^2. Although the type of Si bonding in the high-pressure phase of $CaSi_2$ needs to be confirmed by band-structure calculations, results presented in this work seem to corroborate this empirical rule which is a clear indication for the search of new silicon-based superconductors.

ACKNOWLEDGMENT

We thank Professor S. Massidda (University of Cagliari, Italy) for discussions on the electronic structures of these materials and for sharing with us his preliminary results.

[1] M. Hanfland, U. Schwarz, K. Syassen, and K. Takemura, Phys. Rev. Lett. **82**, 1197 (1999), and references therein.
[2] M. Affronte, O. Laborde, G. L. Olcese, and A. Palenzona, J. Alloys Compd. **274**, 68 (1998).
[3] J. Evers, J. Solid State Chem. **28**, 369 (1979).
[4] S. Fahy and D. R. Hamann, Phys. Rev. B **41**, 7587 (1990).
[5] S. Dick and G. Oehlinger, Z. Kristallogr. - New Cryst. Struct. **213**, 232 (1998).
[6] K. Kusakabe, Y. Tateyama, T. Ogitsu, and S. Tsuneyumi, Rev. High Pressure Sci. Technol. **7**, 193 (1998).
[7] J. Evers, G. Oehlinger, and A. Weiss, Angew. Chem. Int. Ed. Engl. **16**, 659 (1977).
[8] M. Imai, T. Hirano, T. Kikegawa, and O. Shimomura, Phys. Rev. B **55**, 132 (1997); **58**, 11 922 (1998), and references therein.
[9] M. Imai, K. Hirota, and T. Hirano, Physica C **245**, 12 (1995).
[10] S. Sanfilippo, H. Elsinger, M. Núñez-Regueiro, O. Laborde, S. LeFloch, M. Affronte, G. L. Olcese, and A. Palenzona, Phys. Rev. B **61**, 3800 (2000).
[11] H. K. Mao, J. Xu, and P. M. Bell, J. Geophys. Res. **91**, 4673 (1986).
[12] A. P. Hammersley *et al.*, High Press. Res. **14**, 235 (1996).
[13] H. Nakano, S. Yamanaka, and M. Hattori, Solid State Ionics **53-56**, 635 (1992).
[14] O. Bisi, L. Braicovich, C. Carbone, I. Lindau, A. Iandelli, G. L. Olcese, and A. Palenzona, Phys. Rev. B **40**, 10 194 (1989).
[15] S. Massidda (private communication).